Talanta 120 (2014) 362–367

Contents lists available at ScienceDirect

Talanta

journal homepage: www.elsevier.com/locate/talanta

Prussian blue nanoparticles as peroxidase mimetics for sensitive colorimetric detection of hydrogen peroxide and glucose

Weimin Zhang, Diao Ma, Jianxiu Du*

Key Laboratory of Analytical Chemistry for Life Science of Shaanxi Province, School of Chemistry and Chemical Engineering, Shaanxi Normal University, Xi'an 710062, People's Republic of China

ARTICLE INFO

Article history:
Received 22 September 2013
Received in revised form
9 December 2013
Accepted 14 December 2013
Available online 19 December 2013

Keywords:
Prussian blue nanoparticles
Peroxidase-like activity
Colorimetric
Hydrogen peroxide
Glucose

ABSTRACT

Prussian blue nanoparticles (PB NPs) exhibits an intrinsic peroxidase-like catalytic activity towards the hydrogen peroxide (H_2O_2)-mediated oxidation of classical peroxidase substrate 2,2′-azino-bis(3-ethylbenzothiazoline-6-sulfonic acid) diammonium salt to produce a colored product. The catalysis follows Michaelis–Menen kinetics and shows strong affinity for H_2O_2. Using PB NPs as a peroxidase mimetics, a colorimetric method was developed for the detection of 0.05–50.0 μM H_2O_2, with a detection limit of 0.031 μM. When the catalytic reaction of PB NPs was coupled with the reaction of glucose oxidation catalyzed by glucose oxidase, a sensitive and selective colorimetric method for the detection of glucose was realized. The limit of detection for glucose was determined to be as low as 0.03 μM and the linear range was from 0.1 μM to 50.0 μM. The method was successfully applied to the determination of glucose in human serum. Compared with other nanomaterials-based peroxidase mimetics, PB NPs provides 10–100 times higher sensitivity toward the detection of H_2O_2 and glucose. The detection platform developed showed great potential applications in varieties of physiological importance substances when merged with appropriate H_2O_2-producing oxidases.

© 2013 Elsevier B.V. All rights reserved.

1. Introduction

The determination of hydrogen peroxide (H_2O_2) is of great significance in clinical assay and related applications. A variety of the analytes of physiological importance (e.g. glucose, uric acid, etc.) are measured by treating the sample with the corresponding oxidase enzymes; the reaction results in the formation of a stoichiometric amount of H_2O_2. The most common approach to measuring H_2O_2 relies on the oxidation of substrates by H_2O_2, mediated by a peroxidase enzyme (typically horseradish peroxidase, HRP), to produce substances with colored, fluorescent or electroactive properties for detection. HRP as a biological catalyst possesses remarkable advantages of high substrate specificity and high efficiency under mild conditions. However, as a natural enzyme HRP is unstable and easily denatured under extreme conditions (e.g. in strong acidic and basic condition, high temperature) or digested by proteases. Furthermore, the preparation, purification and storage of natural enzymes are usually time-consuming and expensive. To overcome the stability and cost issues of biological catalyst, great efforts have been made to explore efficient mimetics of enzyme; hemin [1,2], hematin [3], porphyrin [4,5], molecular imprinted polymers [6,7], DNAzymes [8,9] have been investigated as the candidates of peroxidase mimetics and shown to be effective.

The application of nanomaterials as the candidates of peroxidase mimetics has recently been of great interest since the work of Yan et al. on intrinsic peroxidase-like activity of Fe_3O_4 magnetic nanoparticles (NPs) [10]. Following their work, some other nanomaterials, including gold NPs [11,12], FeS nano-sheet [13], $CoFe_2O_4$ magnetic NPs [14,15], CuO NPs [16], Co_3O_4 NPs [17], V_2O_5 nanowires [18], carbon nanomaterials [19–21], polyoxometalates [22], and RuO_2 NPs [23] have been discovered to possess intrinsic peroxidase-like activity. The nanomaterials as the peroxidase mimetics have the advantages of low cost, ease of preparation and high stability compared to HRP, which have found many potential applications in biosensing and environmental applications [24,25].

Prussian blue (PB), $Fe_4[Fe(CN)_6]_3$, has been extensively explored as electron transfer mediator for the construction of first-generation oxidase-based electrochemical biosensor due to its excellent electrochemical behavior and good catalytic property [26–28]. Prussian blue contains Fe^{3+}/Fe^{2+} redox couple, the reversible conversion of which occurs in the reaction centers of a number of peroxidase enzymes. More recently the peroxidase-like activity of γ-Fe_2O_3 magnetic NPs was reported to improve significantly after modification with PB [29,30]. However, Prussian blue has not been determined to be a potential peroxidase mimetics. We here demonstrate for the first time that Prussian blue NPs (PB NPs) exhibit intrinsic peroxidase-like activity like HRP. And the PB NPs were successfully

* Corresponding author. Tel.: +86 29 81530726; fax: +86 29 81530727.
E-mail address: jxdu@snnu.edu.cn (J. Du).

0039-9140/$ - see front matter © 2013 Elsevier B.V. All rights reserved.
http://dx.doi.org/10.1016/j.talanta.2013.12.028

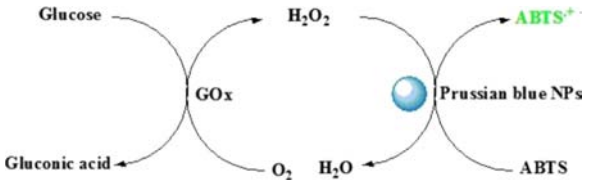

Scheme 1. Schematic illustration of colorimetric detection of H_2O_2 and glucose by Prusian blue nanoparticles and glucose oxidase (GO*x*).

used as peroxidase mimetics for colorimetric detection of H_2O_2 and glucose (Scheme 1).

2. Experimental

2.1. Apparatus

The UV–visible absorption spectra were taken on a TU-1901 spectrophotometer (Beijing Purkinje General Instrument Co. Ltd, China) in the wavelength range of 400–500 nm with a slit width of 2.0 nm. Transmission electron microscopy (TEM) images were obtained on a JEM-2100 transmission electron microscope (Japan Electronic Company, Japan) with an accelerating voltage of 200 kV. Zeta potential was measured on a Delsa Nano C laser particle zeta potential instrument (Beckman Coulter INC, USA) with a solid-state laser (15 W, 659 nm). The pH of the solutions was measured with a pHs-3C precision pH meter (Shanghai Precision Scientific Instruments Co., Ltd., China).

2.2. Chemicals

All chemicals were of analytical grade and used as received without further purification. Doubly distilled de-ionized water was obtained from a SZ-93 automatic de-ionized, distilled water system (Shanghai Yarong Biochemistry Instrument Factory, China). $K_3[Fe(CN)_6]$, $FeCl_2 \cdot 4H_2O$, H_2O_2 (30%, w/w), and D-glucose were purchased from Xi′an Chemical Industry Co. Ltd, China. Glucose oxidase (type X–S from Aspergillums Niger, 50 U/mg) and 2,2′-azino-bis(3-ethylbenzothiazoline-6-dulfonic acid) diammonium salt (ABTS) were purchased from Sigma-Aldrich, USA. D-maltose was obtained from Beijing Aoboxing Bio-tech Co. Ltd, China. D-lactose and D-fructose were obtained from Shanghai Sangon Biological Engineering Technology and Service Co. Ltd, China. The exact concentration of H_2O_2 solution was determined by titration with $KMnO_4$ previously standardized with sodium oxalate.

2.3. Synthesis of PB NPs

The glassware was thoroughly cleaned with aqua regia followed by rinsing with doubly distilled de-ionized water and drying before use. PB NPs were prepared via one step synthesis protocol described elsewhere [31]. An aqueous solution of 1 mM $K_3[Fe(CN)_6]$ (100 mL) was added dropwise into 100 mL of 1 mM $FeCl_2$ solution under vigorous stirring. The color of the solution gradually changed to dark blue, indicating the formation of PB NPs. To remove KCl from the composite, PB NPs were precipitated from the mixture by adding 400 mL of acetone into above-mentioned reaction mixture. The resultant precipitate was separated by centrifugation at 9000 r/min for 30 min and further cleaned with acetone three times. The as-prepared PB NPs solid were re-dissolved in water for use. The concentration of PB NPs solution was calculated by the total Fe concentration in the PB NPs solution determined by atom absorption spectroscopy and its molecular formula of $Fe_4[Fe(CN)_6]_3$.

2.4. H_2O_2 detection with PB NPs as peroxidase mimetics

First, 480 μL of 30 mM ABTS, 150 μL of 5 μM PB NPs, 36 μL of different concentration of H_2O_2 were added into 0.2 M acetate buffer (pH 4.0) to a total volume of 3.645 mL. Second, the mixed solution was incubated at 50 °C for 15 min and then terminated the reaction by cooling to the ambient temperature by the flow of tap water. Finally, the absorbance of the resulting solution at 420 nm was determined and plotted against the H_2O_2 concentration.

2.5. Glucose detection using PB NPs and GO_x

Human blood samples from four volunteers were collected from the Hospital of Shaanxi Normal University. Glucose concentrations in blood samples were first determined in the hospital and then analyzed by this method. Into 0.1 mL of samples, 1.9 mL of H_2O was added, followed with 1.0 mL of 0.05 M $Ba(OH)_2$ solution and 1.0 mL of $ZnSO_4$ solution to remove proteins existed in blood [32]. The mixture was allowed to stand for 5 min and centrifuge at 10000 r/min for 25 min. Forty micro litre of supernatant was mixed with 10 μL of 10 mg/mL GOx solution and incubated at 37 °C for 10 min, and determined by this method. 10 μL of 10 mg/mL GO_x and 40 μL of glucose with different concentration in 25 mM phosphate buffer solution (pH 7.4) were incubated at 37 °C for 10 min. Then 480 μL of 30 mM ABTS, 150 μL of 5 μM PB NPs, 36 μL of above-mentioned mixture of glucose and GO_x were added into 0.2 M acetate buffer (pH 4.0) to a total volume of 3.645 mL. After incubating at 50 °C water bath for 15 min, the reaction was terminated by cooling to the ambient temperature by the flow of tap water. The absorbance of the resulting solution at 420 nm was determined for glucose calibration.

In control experiments, 100.0 μM maltose, 100.0 μM lactose, and 100.0 μM fructose were used in place of glucose following the same procedure.

3. Results and discussion

3.1. Preparation and characterization of PB NPs

Prussian blue NPs were synthesized via one step synthesis protocol as reported by Li et al. [31]. The as-prepared PB NPs solution shows the characteristic Prussian blue color with a broad band centering at 705 nm, which responds to an intermetal charge-transfer band from Fe^{2+} to Fe^{3+} in Prussian blue. TEM images indicate that PB NPs are spherical with an average size about 20 nm (Fig. 1). The value of zeta potential is −4.59, indicating that the surface of PB NPs is negative charged.

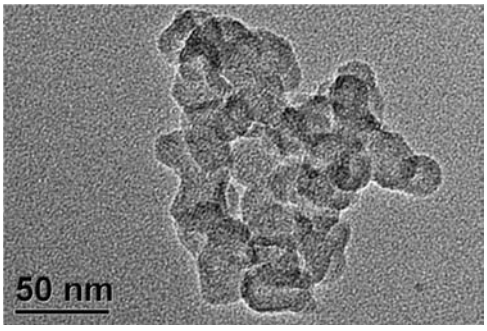

Fig. 1. Transmission electron microscope (TEM) of the as–prepared Prusian blue nanoparticles obtained on JEM–2100 TEM with an accelerating voltage of 200 KV.

3.2. Peroxidase-like activity of PB NPs

The as-prepared PB NPs can catalyze the oxidation of peroxidase substrate ABTS by H_2O_2 to produce ABTS radical cation ($ABTS^{\bullet+}$). The resulting solution shows a green color and has a maximum absorption peak at 420 nm (Fig. 2, solid line). ABTS oxidation also occurs in the presence of H_2O_2 without PB NPs as the catalyst (Fig. 2, dash line), as has been reported by Wei and Wang [33]. But the absorbance of ABTS–H_2O_2 system was significantly lower than that of ABTS–H_2O_2–PB NPs system. The mixture of PB NPs and ABTS showed very poor absorption at this wavelength (Fig. 2, dot line). These results suggested that PB NPs possessed an intrinsic peroxidase-like activity. The effect of supernatant of the PB NPs solution was also examined on the ABTS oxidation reaction. No catalytic reaction was observed by using the supernatant of PB NPs (Fig. 2, short dot line), indicating that the ions generated from leaching process of PB NPs do not have the peroxidase-like catalytic activity.

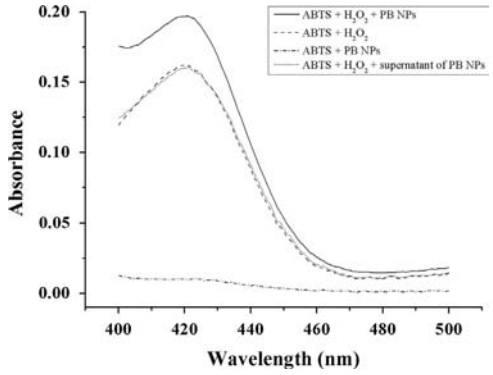

Fig. 2. Typical absorption spectra of (solid line) 2,2′–azino–bis(3–ethylbenzothiazoline–6–sulfonic acid) diammonium salt (ABTS)–H_2O_2–Prusian blue nanoparticles (PB NPs), (dash line) ABTS–H_2O_2, (dot line) ABTS–PB NPs, and (short dot line) ABTS–H_2O_2–the supernatant of PB NPs. The reactions were incubated at 50 °C for 15 min in 0.2 M HAc–NaAc buffer (pH 4.0) with 0.2 μM PB NPs as the catalyst and 4.0 mM ABTS as the substrate. The H_2O_2 concentration was 5.0 μM.

3.3. Catalytic activity of PB NPs against pH and temperature

The catalytic activity of PB NPs is strongly dependent on pH and temperature, similar to HRP and other NPs-based peroxidase mimetics. Fig. 3A showed that Prussian blue NPs had higher catalytic activity under slightly acidic conditions than neutral and alkaline conditions. The maximum catalytic efficiency was obtained at pH 4.0, as has also been observed for V_2O_5 nanowires [18] and HRP [34] with ABTS as the substrate. In the range of 25–65 °C, the optimal temperature was 50 °C (Fig. 3B), which is very similar to that observed with Fe_3O_4 NPs as peroxidase mimetics [33].

3.4. Effect of reaction time

We examined the effect of the reaction time on the catalytic activity in the range of 5–50 min. As shown in Fig. 4, the absorbance at 420 nm was increased with increasing the reaction time up to 15 min. When the reaction time was longer than 15 min, the absorbance

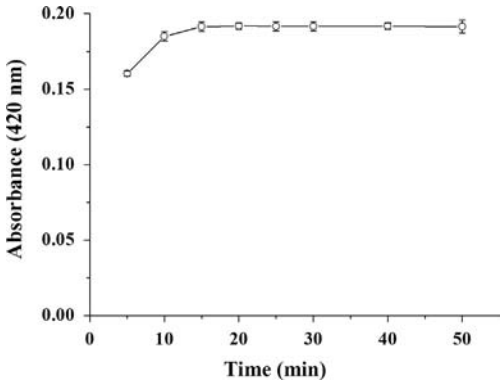

Fig. 4. Effect of reaction time. Experiments were carried out in 3.645 mL 0.2 M HAc–NaAc buffer (pH 4) at 50 °C with 0.2 μM Prusian blue nanoparticles as the catalyst and 4.0 mM 2,2`–azino–bis(3–ethylbenzothiazoline–6–sulfonic acid) diammonium salt as the substrate. The H_2O_2 concentration was 5.0 μM. Error bars indicate the standard deviation for three measurements.

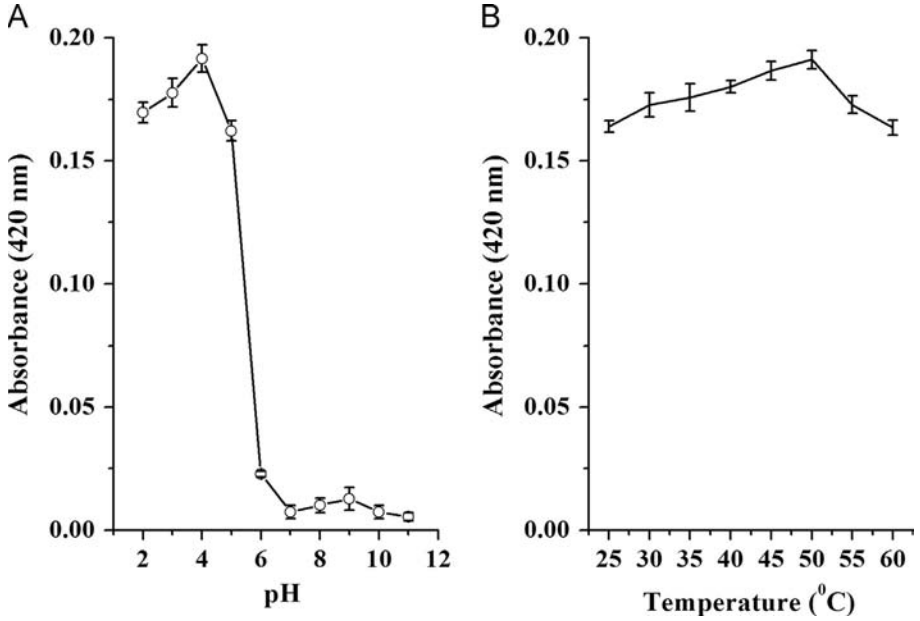

Fig. 3. Catalytic activity of Prusian blue nanoparticles (PB NPs) against (A) pH and (B) temperature. Experiments were carried out in 3.645 mL 0.2 M HAc–NaAc buffer with 0.2 μM PB NPs as the catalyst and 4.0 mM 2,2′–azino–bis(3–ethylbenzothiazoline–6–sulfonic acid) diammonium salt as the substrate. The H_2O_2 concentration was 5.0 μM. Error bars indicate the standard deviation for three measurements.

remained almost the constant. Thus, 15 min was employed as the reaction time.

3.5. Steady-state kinetic assay of PB NPs

To further investigate the kinetic mechanism of the peroxidase-like activity of PB NPs, steady-state kinetic experiments were carried out by varying the concentration of H_2O_2 (2.0–200.0030 μM) and ABTS (0.5–4.0 mM) one at a time while keeping other conditions constant. The absorbance data at 420 nm was used to back-calculate the concentration of $ABTS^{\bullet+}$ using a molar absorption coefficient of 3.6×10^4/(cm M) [35]. The velocity of the reaction at different concentrations of substrate was obtained by calculating the slopes of absorbance changes with time. The catalytic ability of PB NPs on H_2O_2-mediated oxidation of ABTS was dependent on the substrate concentrations and followed Michaelis–Menten behavior towards both H_2O_2 and ABTS (Fig. 5A and B). Michaelis–Menten constants (K_m) were obtained by using Linewaerver–Burk plots (Fig. 5C and D). The apparent K_m value for PB NPs with H_2O_2 as the substrate was 0.028 mM, much lower than that of HRP (0.24 mM) [33], suggesting that PB NPs had higher affinity for H_2O_2 than HRP. On the other hand, the apparent K_m value for PB NPs with ABTS as the substrate was 157.45 mM, significantly higher than that of 1.56 mM for HRP [34], suggesting that PB NPs had lower affinity for ABTS than HRP.

3.6. Determination of H_2O_2 and glucose

Since the catalytic activity of PB NPs is also dependent on the H_2O_2 concentration, this system can be used for the colorimetric detection of H_2O_2. The absorbance of the reaction at 420 nm was proportional to the concentration of H_2O_2 in the range of 0.05–50.0 μM (Fig. 6A) with a correlation coefficient of 0.999. The detection limit ($3s_b/S$) was 0.031 μM H_2O_2. By coupling with glucose oxidase (GO_x)-catalyzing the oxidation of glucose, a colorimetric method for glucose detection was also developed. A typical glucose concentration response curve was depicted in Fig. 6B. The linear range for glucose was from 0.1 to 50.0 μM (r=1.000) and the detection limit ($3s_b/m$) was 0.03 μM. Table 1 summarized the analytical figures of the determination of H_2O_2 and glucose by this method and the previous reported methods using other NPs peroxidase mimetics. As can be seen from Table 1, the detection limits of this method was 1–2 orders of magnitude lower than that obtained by using other NPs peroxidase mimetics.

3.7. Selectivity

To test the selectivity of the detection of glucose, the control experiments were performed by using fructose, lactose, and maltose in place of glucose. As can be seen from Fig. 7, even the concentration of control samples was 10 times larger than that of glucose; the absorbance of glucose was much higher than that of control samples. Thus, these compounds did not interfere with the determination of glucose. Maltose produced slightly higher response than blank probably because a small amount of maltose broke down into glucose by hydrolysis at weak acidic conditions [36].

3.8. Detection of glucose in human serum

To test the practicability of the method, it was applied to the determination of glucose in human serum. The results were shown

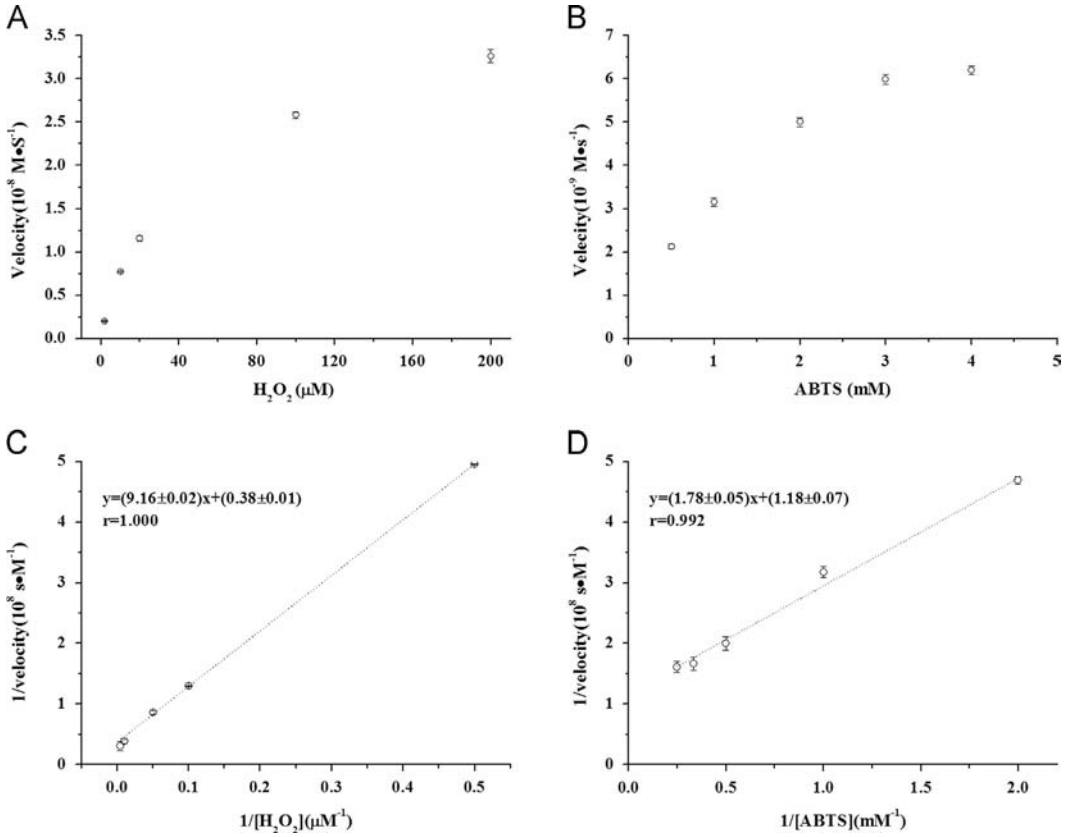

Fig. 5. Steady-state kinetic assay of Prusian blue nanoparticles (PB NPs). Experiments were carried out in 3.645 mL 0.2 M HAc–NaAc buffer at 50 °C for 15 min with 0.2 μM PB NPs as the catalyst. (A) The concentration of 2,2′–azino–bis(3–ethylbenzothiazoline–6–sulfonic acid) diammonium salt (ABTS) was kept at 4.0 mM and the concentration of H_2O_2 was varied from 2.0 to 200.0 μM. (B) The concentration of H_2O_2 was kept at 5.0 μM and the concentration of ABTS was varied from 0.5 to 4.0 mM. (C) and (d) Double-reciprocal plots of activity of PB NPs at a fixed concentration of one substance versus varied concentration of the second substrate for H_2O_2 and ABTS. Error bars indicate the standard deviation for three measurements.

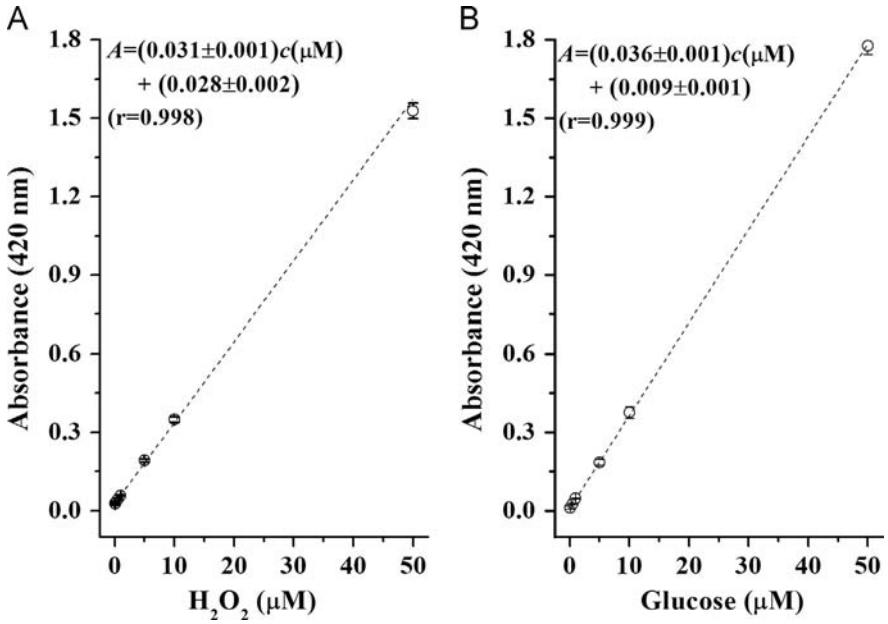

Fig. 6. Linear calibration plot of (A) H2O2 in the range of 0.05–50.0 μM and (B) glucose in the range of 0.1–50.0 μM. Error bars indicate the standard deviation for three measurements. Fig 7. Selectivity of the colorimetric method for glucose detection (from left to right: Blank, 100.0 μM fructose, 100.0 μM lactose, 100.0 μM maltose, and 10.0 μM glucose. Error bars indicate the standard deviation for three measurements.

Table 1
Colorimetric detection of H_2O_2 and glucose with nanomaterials as peroxidase mimics.

Catalysts	Substances	Analytes	Linear range (μM)	Detection limit (μM)	References
(+)Au NPs[a]	TMB[b]	H_2O_2	2–200	0.5	[11]
		Glucose	18–1100	4	
Fe_3O_4 NPs	ABTS[c]	H_2O_2	5–100	3	[32]
		Glucose	5–100	3	
$CoFe_2O_4$ NPs	TMB	Glucose	1.25–18.75	0.3	[15]
Co_3O_4 NPs	TMB	H_2O_2	50–25000	10	[17]
		Glucose	10–10000	5	
C-dots	TMB	H_2O_2	1–100	0.2	[20]
		Glucose	1–500	0.4	
PB NPs	ABTS	H_2O_2	0.05–50.0	0.031	This method
		Glucose	0.1–50.0	0.03	

[a] NPs: nanoparticles.
[b] TMB: 3,3,5,5-tetramethylbenzidine.
[c] ABTS: 2,2′-azino-bis(3-ethylbenzothiazoline-6-sulfonic acid) diammonium salt.

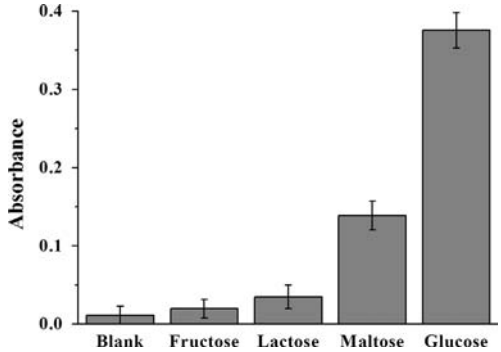

Fig. 7. Selectivity of the colorimetric method for glucose detection (from left to right: Blank, 100.0 μM fructose, 100.0 μM lactose, 100.0 μM maltose, and 10.0 μM glucose. Error bars indicate the standard deviation for three measurements.

Table 2
Determination of glucose in human serum.

Samples	This method (mM ± S.D.) (n=5)	Hospital method (mM) [a]	t-test
No. 1	5.45 ± 0.14	5.60	2.40 < $t_{0.05,5}$ (2.57)
No. 2	5.63 ± 0.11	5.64	0.20 < $t_{0.05,5}$ (2.57)
No. 3	5.34 ± 0.13	5.20	2.41 < $t_{0.05,5}$ (2.57)
No. 4	4.60 ± 0.09	4.62	0.50 < $t_{0.05,5}$ (2.57)

[a] Results obtained by AU480 Chemistry Analyzer (Beckman Coulter).

in Table 2. Student t-test indicated there has no significant difference with that obtained by the hospital method at the confidence level of 95%.

4. Conclusion

In summary, for the first time PB NPs was demonstrated to have the intrinsic peroxidase-like activity. The intrinsic peroxidase-like activity of PB NPs showed typical Michaelis–Menten kinetics and exhibited high catalytic efficiency. By using the peroxidase-like activity of PB NPs, a sensitive and selective colorimetric method was developed for the detection of H_2O_2 and glucose. With the appropriate H_2O_2-producing oxidases, this system can be easily adapted to measure other physiologically important compounds, such as amino acids, uric acid, etc.

Acknowledgements

Financial supports from the Natural Science Foundation of Shaanxi Province (2011JM2004) and Fundamental Research Funds for the Central Universities (GK201302014) are gratefully

acknowledged. The authors gratefully thank the Hospital of Shaanxi Normal University for offering the human serum samples.

References

[1] Q.G. Wang, Z.M. Yang, X.D. Xiao, C.K. Chang, B. Xu, Angew. Chem. Int. Ed. 46 (2007) 4285.
[2] Q.Z. Zhu, F.H. Liu, J.G. Xu, J.W. Huang, Fresenius J. Anal. Chem. 362 (1998) 537.
[3] G.F. Zhang, P.K. Dasgupta, Anal. Chem. 64 (1992) 517.
[4] R.A.W. Johnstone, A.J. Simpson, P.A. Stocks, Chem. Commun. 23 (1997) 2277.
[5] J.Y. Liu, X.F. Li, Z.X. Guo, Y.Z. Li, A.J. Huang, W.B. Chang, J. Mol. Catal. A: Chem. 179 (2002) 27.
[6] W. de Jesus Rodrigues Santos, P.R. Lima, C.R.T. Tarley, L.T. Kubota, Anal. Bioanal. Chem. 389 (2007) 1919.
[7] Z. Chen, L. Xu, Y. Liang, M. Zhao, Adv. Mater. 22 (2010) 1488.
[8] Y.F. Li, D. Sen, Biochemistry 36 (1997) 5589.
[9] J. Kosman, B. Juskowiak, Anal. Chim. Acta 707 (2011) 7.
[10] L.Z. Gao, J. Zhuang, L. Nie, J.B. Zhang, Y. Zhang, N. Gu, T.H. Wang, J. Feng, D. L. Yang, S. Perrett, X. Yan, Nat. Nanotechnol. 2 (2007) 577.
[11] Y. Jv, B.X. Li, R. Cao, Chem. Commun. 46 (2010) 8017.
[12] X.X. Wang, Q. Wu, Z. Shan, Q.M. Huang, Biosens. Bioelectron. 26 (2011) 3614.
[13] Z.H. Dai, S.H. Liu, J.C. Bao, H.X. Ju, Chem. Eur. J. 15 (2009) 4321.
[14] W.B. Shi, X.D. Zhang, S.H. He, Y.M. Huang, Chem. Commun. 47 (2011) 10785.
[15] L. Su, J. Feng, X.M. Zhou, C.L. Ren, H.H. Li, X.G. Chen, Anal. Chem. 84 (2012) 5753.
[16] W. Chen, J. Chen, A.L. Liu, L.M. Wang, G.W. Li, X.H. Lin, ChemCatChem 3 (2011) 1151.
[17] J.S. Mu, Y. Wang, M. Zhao, L. Zhang, Chem. Commun. 48 (2012) 2540.
[18] R. Andre, F. Natalio, M. Humanes, J. Leppin, K. Heinze, R. Wever, H.C. Schroder, W.E.G. Mueller, W. Tremel, Adv. Funct. Mater. 21 (2011) 501.
[19] Y.J. Song, X.H. Wang, C. Zhao, K.G. Qu, J.S. Ren, X.G. Qu, Chem. Eur. J. 16 (2010) 3617.
[20] W.B. Shi, Q.L. Wang, Y.J. Long, Z.L. Cheng, S.H. Chen, H.Z. Zheng, Y.M. Huang, Chem. Commun. 47 (2011) 6695.
[21] F.L. Qu, T. Li, M.H. Yang, Biosens. Bioelectron. 26 (2011) 3927.
[22] J.J. Wang, D.X. Han, X.H. Wang, B. Qi, M.S. Zhao, Biosens. Bioelectron. 46 (2012) 18.
[23] H.M. Deng, W. Shen, Y.F. Peng, X.J. Chen, G.S. Yi, Z.Q. Gao, Chem. Eur. J. 18 (2012) 8906.
[24] Y. Song, W Wei, X. Qu, Adv. Mater. 23 (2011) 4215.
[25] J. Xie, X. Zhang, H. Wang, H. Zheng, Y. Huang, TrAC, Trends Anal. Chem. 39 (2012) 115.
[26] A.A. Karyakin, O.V. Gitelmacher, E.E. Karyakina, Anal. Chem. 67 (1995) 2419.
[27] F. Ricci, G. Palleschi, Biosens. Bioelectron. 21 (2005) 389.
[28] A.V. Mokrushina, M. Heim, E.E. Karyakina, A. Kuhn, A.A. Karyakin, Electrochem. Commun. 29 (2013) 78.
[29] X.Q. Zhang, S.W. Gong, Y. Zhang, T. Yang, C.Y. Wang, N. Gu, J. Mater. Chem. 20 (2010) 5110.
[30] H. Wang, Y.M. Huang, J. Hazard. Mater. 191 (2011) 163.
[31] Q. Zhang, L. Zhang, J.H. Li, J. Nanosci. Nanotechnol. 7 (2007) 4557.
[32] D.T. Bostick, D.M. Hercules, Anal. Chem. 47 (1975) 447.
[33] H. Wei, E. Wang, Anal. Chem. 80 (2008) 2255.
[34] V.H. Gallati, J. Clin. Chem. Clin. Biochem. 17 (1979) 1.
[35] K.S. Shin, Y.J. Lee, Arch. Biochem. Biophys. 384 (2000) 109.
[36] Y.B. Tewari, R.N. Goldberg, J. Biol. Chem. 264 (1989) 3966.